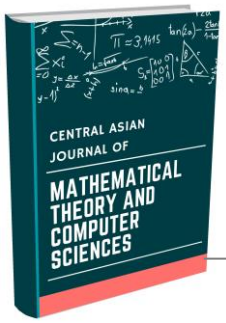

CENTRAL ASIAN JOURNAL OF MATHEMATICAL THEORY AND COMPUTER SCIENCES
http://cajmtcs.centralasianstudies.org/index.php/CAJMTCS
Volume: 03 Issue: 06 | Jun 2022 ISSN: 2660-5309

Convection with Double-Diffusion in an Oscillatory Porous Boundary and a Concentration-Based Internal Heat Source

L. Ebiwareme
Department of Mathematics, Rivers State University, Nigeria
K. W. Bunonyo
MMDARG, Department of Mathematics and Statistics, Federal University Otuoke, Nigeria
O. A. Davies
Department of Physics, Rivers State University, Nigeria

Annotation:
This research was carried out to investigate double-diffusion convection in an oscillatory porous boundary with a concentration-based internal heat source. The models governing the flow were scaled to be dimensionless with the help of the dimensionless quantities. The dimensionless partial differential equations were reduced to ordinary differential equations with the aid of perturbation parameters, and the ODEs have been solved analytically where the temperature, concentration, and velocity profiles were obtained. In the course of scaling and solving the governing system of the equation, we obtained some pertinent parameters with which we carried out numerical simulation using Wolfram Mathematica by varying the parameters such as thermal Rayleigh number, solutal Rayleigh number, Lewis number, Darcy number, magnetic field parameter, Prandtl number, heat source parameter, and oscillatory frequency parameter within a bounded domain. In conclusion, it is seen in the research that varying the pertinent parameters has an impact on the various flow profiles.

ARTICLEINFO

Article history:
Received 18 Apr 2022
Revised form 15 May 2022
Accepted 20 Jun 2022

Key words: Oscillatory flow, Double-Diffusion, Heat Source, ODE, Concentration, and Velocity profile, Temperature profile, Convection, Lewis Number.

---

1. Introduction

When a fluid saturated porous layer confined between two infinite parallel plates containing two substances with different rates of diffusion is heated and salted below, a threshold temperature is reached where the warmer fluid at the bottom expands and becomes lighter and moves to replace the colder fluid at the top, thus creating a convection current. These currents originate when a body force acts on the fluid due to density gradients. The force which induces this convection current is called buoyancy, and the phenomenon

is called double-diffusive or thermosolutal convection. Copious literature has been devoted to studying this phenomenon. Pioneer studies on the subject are credited to Lord Rayleigh in his trail-blazing experiment in 1916. Chandrasekhar [1] advanced conditions leading to the onset of stability for both stationary and oscillatory convection for free-free, free-rigid, and rigid-rigid boundaries. To predict the conditions leading to the onset of instability, several methods have been applied to certain degrees of accuracy, which validates experimental results. Some of these methods include Galerkin, normal mode analysis, perturbation, and energy methods. Many of the industrial applications of double diffusion convection include electrochemistry, crystal growth, petroleum reservoirs, magma chambers, insulation engineering, coal combustors, nuclear reactors, food processing, reservoir modelling, thermal insulation [2-3].

Comprehensive studies have been done on double-diffusive convection and can be found in books by Ingham and Pope [4], Nieldand Bejan [5], Batchelor [6], Drazin & Reid [7], Charru [8], Schmid & Heningson [9], Horton and Rogers [10], Wooding [11], Vafai [12]. Hill [13] analysed double diffusive convection in a porous medium with a concentration-based internal heat source using the Darcy and Boussinesq approximation. In this study, it was assumed that the porous boundaries are insulated, and the magnetic field is assumed to be small. The equation of state is taken to be linear with temperature and concentration. When the thermal Rayleigh number is less or equal to the heat source parameter, no oscillatory convection occurs. Compared to comparing the linear and nonlinear thresholds using the linear stability analysis and energy method, the findings showed that irrespective of the magnitude of the heat source parameter, the threshold remains unchanged even when the solutal Rayleigh number is increased.

Gaikwad and Dhanraj [14] have examined the onset of double-diffusive reaction-convection in an anisotropic porous layer with an internal heat source. In this study, the boundaries of the wall are subjected to chemical equilibrium and the effects of thermal Rayleigh number, Damkohler number, thermal anisotropic parameter, internal heat parameter, and mechanical anisotropy parameter are to destabilize the system, thereby hastening the onset of instability, while the system is stabilized in the presence of thermal anisotropy parameter for both the stationary and oscillatory modes. Similarly, the presence of Damkohler number has a destabilizing effect on the stationary mode, while for the oscillatory mode; it delays the onset of instability and stabilizes the system.

Israel-Cookey *et al*. [15] have studied the simultaneous effects of a vertical magnetic field and a concentration-based internal heat source on the onset of double-diffusive convection in a horizontal porous medium using the linear stability analysis technique. The study revealed the Hartmann and solutal Rayleigh numbers delay the onset of instability for both stationary and oscillatory convection, while the Lewis number stabilizes the system for stationary and hastens instability only for the oscillatory mode. The Lewis number destabilizes the system for oscillatory convection, whereas heat source parameters lead to a destabilization of the system for both stationary and oscillatory convection.

Hill [16] has investigated the thermal instability of double-diffusive convection in an inclined porous layer with a concentration-based internal heat source. It was shown in this study that stabilization of the system was achieved with an increase in the angle of inclination for the transverse rolls, the magnitude of the vertical solutal Rayleigh number and internal heat source parameter.

Israel-Cookey *et al*. [17] examined the combined effects of Soret and magnetic field on thermosolutal convection in a porous medium with a concentration-based internal heat source. The study showed that the effect of magnetic field is to delay the onset of instability for both modes. Soret destabilizes the system and for ranges of the heat source parameter less than, the system is stable; whereas, for values greater than or equal to, the system becomes unstable for all values of Soret and magnetic field.

Kumar et al. [18] studied the linear and nonlinear thermosolutal instabilities in an inclined porous layer with a concentration-based internal heat source. Subcritical instability regions were obtained when the linear and nonlinear thresholds for longitudinal and transverse rolls were compared. Instability of the system is

hastened when the thermal diffusivity is greater than the solute and internal heat source. However, an increase in the angle of inclination stabilizes the system, which delays the onset of instability.

Ebiwareme and Israel-Cookey [19] investigated the onset of Darcy-Brinkmann convection in a thin, porous layer with concentration-based internal heating with magnetic field effects utilizing the normal mode analysis technique. The findings of this study revealed that stabilization of the system is achieved in the presence of Vadasz and Darcy numbers, while the heat source parameter hastened instability in the system for both stationary and oscillatory convection.

Most recently, Odok et al. [20] have considered the onset of magneto-convection in a rotating Darcy-Brinkmann porous layer heated from below with a temperature-dependent heat source using linear stability analysis for free-free boundaries. The effects of rotation, magnetic field, heat source, Prandtl number, and ratio of viscosities for both stationary and oscillatory convection are analysed and presented graphically. The study shows the rotation, magnetic field, and ratio of viscosities delay the onset of both stationary and oscillatory convection. The internal heat source parameter destabilizes the system while the onset of instability is slowed with the presence of Prandtl number.

Our motivation in this present study is to extend the novelty of obtaining the velocity and temperature profiles for momentum, energy, and specie concentration equations by assuming oscillatory boundary conditions. The effects of the pertinent parameters on the different profiles are presented in tables and graphs. The organization of the study is as follows. Section 1 gives a detailed review of double-diffusive convection in a porous layer with a concentration-based internal heat source. The basic governing equations of the MHD flow subject to the prescribed oscillatory boundary condition are presented in Section Two. Section three gives the detailed mathematical analysis of the problem to give the different profiles for momentum, energy, and concentration profiles. The results of the obtained solution as presented graphically for different values of the model parameters are contained in section four. The discussion of the impact of the various parameters on the different profiles is given in section five. Concluding remarks are given in section six.

2 Mathematical Formulation

We shall present the models governing the fluid flow through porous boundaries by following Issrael-Cookey *et al.*[17], which are

2.1 Continuity Equation

$$\nabla^* \vec{w} = 0 \tag{1}$$

2.2 Momentum Equation

$$\frac{A\rho_0}{\phi_1}\frac{\partial \vec{w}^*}{\partial t^*} = -\frac{\partial P^*}{\partial x^*} - \frac{\mu}{k}\vec{w}^* + \vec{J}\times\vec{B} - \rho\left(T^*, C^*\right)g\vec{k} \tag{2}$$

2.3 Energy Equation

$$A\frac{\partial T^*}{\partial t^*} + \left(\vec{w}^*.\nabla^*\right)T^* = \alpha_T \frac{\partial^2 T^*}{\partial y^{*2}} + Q\left(C^* - C_0\right) \tag{3}$$

2.4 Specie Concentration Equation

$$\phi_1\frac{\partial C^*}{\partial t^*} + \left(\vec{w}^*.\nabla^*\right)C^* = D_c\frac{\partial^2 C^*}{\partial y^{*2}} \tag{4}$$

Boussinesq Approximation

$$\rho\left(T^*,C^*\right)=\rho_0\left[1-\beta_T\left(T^*-T_0\right)+\beta_C\left(C^*-C_0\right)\right] \tag{5}$$

$$\vec{J}=\sigma_c\left(\vec{E}^*+\vec{w}^*\times\vec{B}^*\right),\nabla.\vec{J}=0 \tag{6}$$

where $A=\dfrac{\left(\rho c_p\right)_m}{\left(\rho c_p\right)_f},\alpha_T=\dfrac{k_T}{\left(\rho c_p\right)_f},Q=\dfrac{\beta}{\left(\rho c_p\right)_f}$

The boundary conditions are:

$$\left.\begin{aligned} &w^*=0,T^*=T_0+\left(\frac{T_1-T_2}{2}\right),C^*=C_0+\left(\frac{C_1-C_2}{2}\right) && \text{at } y^*=h\\ &w^*=0,T^*=T_0,C^*=C_0 && \text{at } y^*=0\end{aligned}\right\} \tag{7}$$

Assuming the fluid flow has no electrical conductivity, then $\vec{E}^*=0,\vec{B}=\left(0,B_0,0\right)$

Following Israel-Cookey *et al*. (2017), the curl of the current and the magnetic field becomes

$$\vec{J}=\sigma_c\left(\vec{w}^*\times\vec{B}^*\right)=-\sigma_c B_0^2 w \tag{8}$$

Using the following nondimensional variables

$$\left.\begin{aligned} &\left(x,y\right)=\frac{\left(x^*,y^*\right)}{h},t=\frac{\alpha_T}{Ah^2}t^*,w=\frac{h}{\alpha_T}\vec{w}^*,\theta=\sqrt{Ra}\left(\frac{T^*-T_0}{\delta_T}\right),\phi=\sqrt{Ra}\left(\frac{C^*-C_0}{\delta_C}\right)\\ &\delta_C=C_1-C_2,\delta_T=T_1-T_2,P=\frac{k}{\mu\alpha_T}\left(P^*+\rho_0 gy\right),\varepsilon=\frac{\phi_1}{A}\end{aligned}\right\} \tag{9}$$

Substituting equation (9) into equations (1)-(4), we have:

$$\nabla.w=0 \tag{10}$$

$$\left(\frac{Da}{Pr\phi_1}\right)\frac{\partial w}{\partial t}=-\frac{\partial P}{\partial x}+\sqrt{Ra}\theta-M^2w+Rs\phi \tag{11}$$

$$\frac{\partial\theta}{\partial t}=\frac{1}{Le}\frac{\partial^2\theta}{\partial y^2}+\sqrt{Ra}\gamma \tag{12}$$

$$\varepsilon\frac{\partial\phi}{\partial t}=\frac{1}{Le}\frac{\partial^2\phi}{\partial y^2} \tag{13}$$

The subjected boundary conditions are:

$$\left.\begin{aligned} &w=0,\theta=0,\phi=0 && \text{at } y=0\\ &w=0,\theta=\frac{\sqrt{Ra}}{2},\phi=\frac{\sqrt{Ra}}{2} && \text{at } y=1\end{aligned}\right\} \tag{14}$$

where the governing parameters becomes

$$\left.\begin{aligned} &Ra=\sqrt{\frac{\rho_0 g\beta_T kh\delta_T}{\mu\alpha_T}}, Rs=\frac{\rho_0 g\beta_C kh\delta_C}{\mu\alpha_T}, M=\sqrt{\frac{k\sigma_C B_0^2}{\mu}}, Le=\frac{\alpha_T}{h^2},\\ &\gamma=\frac{h^2 Q\delta_C}{\alpha_T\delta_T}, Pr=\frac{\mu}{\rho_0\alpha_T}, Va=\frac{Pr\phi_1}{Da}, \varepsilon=\frac{\phi_1}{A}, Da=\frac{k}{h^2}\end{aligned}\right\} \quad (15)$$

3 Analytical Solution

Since the flow is through an oscillatory porous boundary, It is assumed that the solution is in the following form:

$$\left.w=w_0 e^{\omega t}, \theta=\theta_0 e^{\omega t}, \phi=\phi_0 e^{\omega t}\right\} \quad (16)$$

Differentiate equation (16) accordingly and substitute the result into equations (11)-(14), we have

$$\left(\left(\frac{Da\omega}{Pr\phi_1}\right)+M^2\right)w_0-\sqrt{Ra}\theta_0-Rs\phi_0=-P \quad (17)$$

$$\frac{\partial^2\theta_0}{\partial y^2}-\beta_2\theta_0=-\sqrt{Ra}Le\gamma e^{-\omega t} \quad (18)$$

where $\beta_2=\omega Le$

$$\frac{\partial^2\phi_0}{\partial y^2}-\beta_1\phi_0=0 \quad (19)$$

where $\beta_1=\varepsilon\omega Le$

The subjected boundary conditions are:

$$\left.\begin{aligned} &w_0=0, \theta_0=0, \phi_0=0 && \text{at } y=0\\ &w_0=0, \theta_0=\frac{\sqrt{Ra}}{2}e^{-\omega t}, \phi_0=\frac{\sqrt{Ra}}{2}e^{-\omega t} && \text{at } y=1\end{aligned}\right\} \quad (20)$$

Solving equation (19), we have

$$\phi_0(y)=Ae^{\left(\sqrt{\beta_1}y\right)}+Be^{-\left(\sqrt{\beta_1}y\right)} \quad (21)$$

Solving equation (21) using the boundary condition in equation (20), we obtain the coefficients as:

$$A=\frac{\sqrt{Ra}e^{-\omega t}}{2\left(e^{\left(\sqrt{\beta_1}\right)}-e^{-\left(\sqrt{\beta_1}\right)}\right)}, B=\frac{\sqrt{Ra}e^{-\omega t}}{2\left(e^{-\left(\sqrt{\beta_1}\right)}-e^{\left(\sqrt{\beta_1}\right)}\right)} \quad (22)$$

We substitute equation (22) into equation (21), so that it becomes:

$$\phi_0(y)=\left(\frac{\sqrt{Ra}e^{-\omega t}}{2\left(e^{\left(\sqrt{\beta_1}\right)}-e^{-\left(\sqrt{\beta_1}\right)}\right)}\right)e^{\left(\sqrt{\beta_1}y\right)}+\left(\frac{\sqrt{Ra}e^{-\omega t}}{2\left(e^{-\left(\sqrt{\beta_1}\right)}-e^{\left(\sqrt{\beta_1}\right)}\right)}\right)e^{-\left(\sqrt{\beta_1}y\right)} \quad (23)$$

To get the temperature distribution, we shall solving equation (18), and the result obtained

$$\theta_0(y) = A_2 e^{\sqrt{\beta_2} y} + B_2 e^{-\sqrt{\beta_2} y} + \frac{\sqrt{Ra}Le\gamma}{\beta_2} e^{-\omega t} \tag{24}$$

Solving for the constant coefficients in equation (24) using the corresponding boundary conditions in equation (20), which is

$$A_2 + B_2 = -\frac{\sqrt{Ra}Le\gamma}{\beta_2} e^{-\omega t} \tag{25}$$

$$A_2 e^{\sqrt{\beta_2}} + B_2 e^{-\sqrt{\beta_2}} = \left(\frac{\sqrt{Ra}}{2} - \frac{\sqrt{Ra}Le\gamma}{\beta_2} \right) e^{-\omega t} \tag{26}$$

Presenting equation (18) in matrix form, we have:

$$\begin{pmatrix} 1 & 1 \\ e^{\sqrt{\beta_2}} & e^{-\sqrt{\beta_2}} \end{pmatrix} \begin{pmatrix} A_2 \\ B_2 \end{pmatrix} = \begin{pmatrix} -\frac{\sqrt{Ra}Le\gamma}{\beta_2} e^{-\omega t} \\ \left(\frac{\sqrt{Ra}}{2} - \frac{\sqrt{Ra}Le\gamma}{\beta_2} \right) e^{-\omega t} \end{pmatrix} \tag{27}$$

Let $\alpha_2 = -\frac{\sqrt{Ra}Le\gamma}{\beta_2} e^{-\omega t}$ and $\alpha_3 = \left(\frac{\sqrt{Ra}}{2} - \frac{\sqrt{Ra}Le\gamma}{\beta_2} \right) e^{-\omega t}$ so that equation (27) reduces to:

$$\begin{pmatrix} 1 & 1 \\ e^{\sqrt{\beta_2}} & e^{-\sqrt{\beta_2}} \end{pmatrix} \begin{pmatrix} A_2 \\ B_2 \end{pmatrix} = \begin{pmatrix} \alpha_2 \\ \alpha_3 \end{pmatrix} \tag{28}$$

$$\Delta_0 = \begin{vmatrix} 1 & 1 \\ e^{\sqrt{\beta_2}} & e^{-\sqrt{\beta_2}} \end{vmatrix} = \left(e^{-\sqrt{\beta_2}} - e^{\sqrt{\beta_2}} \right) \tag{28}$$

$$\Delta_1 = \begin{vmatrix} \alpha_2 & 1 \\ \alpha_3 & e^{-\sqrt{\beta_2}} \end{vmatrix} = \alpha_2 e^{-\sqrt{\beta_2}} - \alpha_3 \tag{29}$$

$$\Delta_2 = \begin{vmatrix} 1 & \alpha_2 \\ e^{\sqrt{\beta_2}} & \alpha_3 \end{vmatrix} = \alpha_3 - \alpha_2 e^{\sqrt{\beta_2}} \tag{30}$$

$$A_2 = \frac{\alpha_2 e^{-\sqrt{\beta_2}} - \alpha_3}{\left(e^{-\sqrt{\beta_2}} - e^{\sqrt{\beta_2}}\right)} \text{ and } B_2 = \frac{\alpha_3 - \alpha_2 e^{\sqrt{\beta_2}}}{\left(e^{-\sqrt{\beta_2}} - e^{\sqrt{\beta_2}}\right)} \tag{31}$$

Substitute equation (31) into equation (24), we obtain:

$$\theta_0(y) = \left(\frac{\alpha_2 e^{-\sqrt{\beta_2}} - \alpha_3}{\left(e^{-\sqrt{\beta_2}} - e^{\sqrt{\beta_2}}\right)}\right) e^{\sqrt{\beta_2} y} + \left(\frac{\alpha_3 - \alpha_2 e^{\sqrt{\beta_2}}}{\left(e^{-\sqrt{\beta_2}} - e^{\sqrt{\beta_2}}\right)}\right) e^{-\sqrt{\beta_2} y} + \frac{\sqrt{Ra}Le\gamma}{\beta_2} e^{-\omega t} \tag{32}$$

To obtain the fluid velocity profile, shall substitute equations (23) and (32) into equation (17), which is

To obtain the fluid velocity, we substitute equations (23) – (32) into equation (17), we obtain:

$$\left(\left(\frac{Da\omega}{Pr\phi_1}\right) + M^2\right) w_0 - \sqrt{Ra}\left(A_2 e^{\sqrt{\beta_2} y} + B_2 e^{-\sqrt{\beta_2} y} + \frac{\sqrt{Ra}Le\gamma}{\beta_2} e^{-\omega t}\right) - Rs\left(Ae^{\left(\sqrt{\beta_1} y\right)} + Be^{-\left(\sqrt{\beta_1} y\right)}\right) = -P \tag{33}$$

where all constants coefficients in equation (33) remain as mentioned above.

Solving for the velocity, we have

$$w_0 = \left(\begin{array}{l} \dfrac{\sqrt{Ra}}{\left(\left(\dfrac{Da\omega}{Pr\phi_1}\right) + M^2\right)}\left(A_2 e^{\sqrt{\beta_2} y} + B_2 e^{-\sqrt{\beta_2} y} + \dfrac{\sqrt{Ra}Le\gamma}{\beta_2} e^{-\omega t}\right) + \\ \dfrac{Rs}{\left(\left(\dfrac{Da\omega}{Pr\phi_1}\right) + M^2\right)}\left(Ae^{\left(\sqrt{\beta_1} y\right)} + Be^{-\left(\sqrt{\beta_1} y\right)}\right) - \dfrac{P}{\left(\left(\dfrac{Da\omega}{Pr\phi_1}\right) + M^2\right)} \end{array}\right) \tag{34}$$

But if we substitute the constants into equation (34), we have:

$$\begin{array}{l} \left(\left(\dfrac{Da\omega}{Pr\phi_1}\right) + M^2\right) w_0 - \sqrt{Ra}\left(\left(\dfrac{\alpha_2 e^{-\sqrt{\beta_2}} - \alpha_3}{\left(e^{-\sqrt{\beta_2}} - e^{\sqrt{\beta_2}}\right)}\right) e^{\sqrt{\beta_2} y} + \left(\dfrac{\alpha_3 - \alpha_2 e^{\sqrt{\beta_2}}}{\left(e^{-\sqrt{\beta_2}} - e^{\sqrt{\beta_2}}\right)}\right) e^{-\sqrt{\beta_2} y} + \dfrac{\sqrt{Ra}Le\gamma}{\beta_2} e^{-\omega t}\right) \\ -Rs\left(\left(\dfrac{\sqrt{Ra}e^{-\omega t}}{2\left(e^{\left(\sqrt{\beta_1}\right)} - e^{-\left(\sqrt{\beta_1}\right)}\right)}\right) e^{\left(\sqrt{\beta_1} y\right)} + \left(\dfrac{\sqrt{Ra}e^{-\omega t}}{2\left(e^{-\left(\sqrt{\beta_1}\right)} - e^{\left(\sqrt{\beta_1}\right)}\right)}\right) e^{-\left(\sqrt{\beta_1} y\right)}\right) = -P \end{array} \tag{35}$$

Solving for the perturbed velocity profile in equation (35), we have:

$$w_0 = \left[\begin{array}{l} \dfrac{P}{\left(\left(\dfrac{Da\omega}{Pr\phi_1}\right)+M^2\right)} - \dfrac{\sqrt{Ra}}{\left(\left(\dfrac{Da\omega}{Pr\phi_1}\right)+M^2\right)}\left(\left(\dfrac{\alpha_2 e^{-\sqrt{\beta_2}}-\alpha_3}{\left(e^{-\sqrt{\beta_2}}-e^{\sqrt{\beta_2}}\right)}\right)e^{\sqrt{\beta_2}y}+\left(\dfrac{\alpha_3-\alpha_2 e^{\sqrt{\beta_2}}}{\left(e^{-\sqrt{\beta_2}}-e^{\sqrt{\beta_2}}\right)}\right)e^{-\sqrt{\beta_2}y}+\dfrac{\sqrt{Ra}Le\gamma}{\beta_2}e^{-\omega t}\right) \\ -\dfrac{Rs}{\left(\left(\dfrac{Da\omega}{Pr\phi_1}\right)+M^2\right)}\left(\left(\dfrac{\sqrt{Ra}e^{-\omega t}}{2\left(e^{\left(\sqrt{\beta_1}\right)}-e^{-\left(\sqrt{\beta_1}\right)}\right)}\right)e^{\left(\sqrt{\beta_1}y\right)}+\left(\dfrac{\sqrt{Ra}e^{-\omega t}}{2\left(e^{-\left(\sqrt{\beta_1}\right)}-e^{\left(\sqrt{\beta_1}\right)}\right)}\right)e^{-\left(\sqrt{\beta_1}y\right)}\right) \end{array} \right] \quad (36)$$

Having obtained the perturbed solutions for concentration, temperature and velocity profiles, we shall substitute equations (24), (32), (35) and (36) into equation (16), which is

$$\phi_0(y) = \left(\frac{\sqrt{Ra}e^{-\omega t}}{2\left(e^{\left(\sqrt{\beta_1}\right)}-e^{-\left(\sqrt{\beta_1}\right)}\right)}\right)e^{\left(\sqrt{\beta_1}y\right)} + \left(\frac{\sqrt{Ra}e^{-\omega t}}{2\left(e^{-\left(\sqrt{\beta_1}\right)}-e^{\left(\sqrt{\beta_1}\right)}\right)}\right)e^{-\left(\sqrt{\beta_1}y\right)} \quad (37)$$

$$\theta_0(y) = \left(\frac{\alpha_2 e^{-\sqrt{\beta_2}}-\alpha_3}{\left(e^{-\sqrt{\beta_2}}-e^{\sqrt{\beta_2}}\right)}\right)e^{\sqrt{\beta_2}y} + \left(\frac{\alpha_3-\alpha_2 e^{\sqrt{\beta_2}}}{\left(e^{-\sqrt{\beta_2}}-e^{\sqrt{\beta_2}}\right)}\right)e^{-\sqrt{\beta_2}y} + \frac{\sqrt{Ra}Le\gamma}{\beta_2}e^{-\omega t} \quad (38)$$

$$w_0 = \left[\begin{array}{l} \dfrac{P}{\left(\left(\dfrac{Da\omega}{Pr\phi_1}\right)+M^2\right)} - \dfrac{\sqrt{Ra}}{\left(\left(\dfrac{Da\omega}{Pr\phi_1}\right)+M^2\right)}\left(A_2 e^{\sqrt{\beta_2}y}+B_2 e^{-\sqrt{\beta_2}y}+\dfrac{\sqrt{Ra}Le\gamma}{\beta_2}e^{-\omega t}\right) \\ -\dfrac{Rs}{\left(\left(\dfrac{Da\omega}{Pr\phi_1}\right)+M^2\right)}\left(Ae^{\left(\sqrt{\beta_1}y\right)}+Be^{-\left(\sqrt{\beta_1}y\right)}\right) \end{array} \right] \quad (39)$$

$$w(y,t) = \left[\begin{array}{l} \dfrac{Pe^{\omega t}}{\left(\left(\dfrac{Da\omega}{Pr\phi_1}\right)+M^2\right)} + \dfrac{e^{\omega t}\sqrt{Ra}}{\left(\left(\dfrac{Da\omega}{Pr\phi_1}\right)+M^2\right)}\left(\left(\dfrac{\alpha_2 e^{-\sqrt{\beta_2}}-\alpha_3}{\left(e^{-\sqrt{\beta_2}}-e^{\sqrt{\beta_2}}\right)}\right)e^{\sqrt{\beta_2}y}+\left(\dfrac{\alpha_3-\alpha_2 e^{\sqrt{\beta_2}}}{\left(e^{-\sqrt{\beta_2}}-e^{\sqrt{\beta_2}}\right)}\right)e^{-\sqrt{\beta_2}y}+\dfrac{\sqrt{Ra}Le\gamma}{\beta_2}e^{-\omega t}\right) \\ +\dfrac{Rse^{\omega t}}{\left(\left(\dfrac{Da\omega}{Pr\phi_1}\right)+M^2\right)}\left(\left(\dfrac{\sqrt{Ra}e^{-\omega t}}{2\left(e^{\left(\sqrt{\beta_1}\right)}-e^{-\left(\sqrt{\beta_1}\right)}\right)}\right)e^{\left(\sqrt{\beta_1}y\right)}+\left(\dfrac{\sqrt{Ra}e^{-\omega t}}{2\left(e^{-\left(\sqrt{\beta_1}\right)}-e^{\left(\sqrt{\beta_1}\right)}\right)}\right)e^{-\left(\sqrt{\beta_1}y\right)}\right) \end{array} \right] \quad (40)$$

4 Results

In this section, numerical computation was performed using computational software called Wolfram Mathematica, version 12. The simulation was done by varying some of the pertinent parameters involved in the analytical solutions. The parameters are derived from Israel-Cookey *et al.* [17], and are in ranges: $0 \le M \le 5, 0 \le \gamma \le 1, 0 \le Da \le 2, 0 \le Pr \le 5,\ Rs = 50\ 0 \le Le \le 3,$

$10 \le Ra \le 50$. The graphical results are presented as follows:

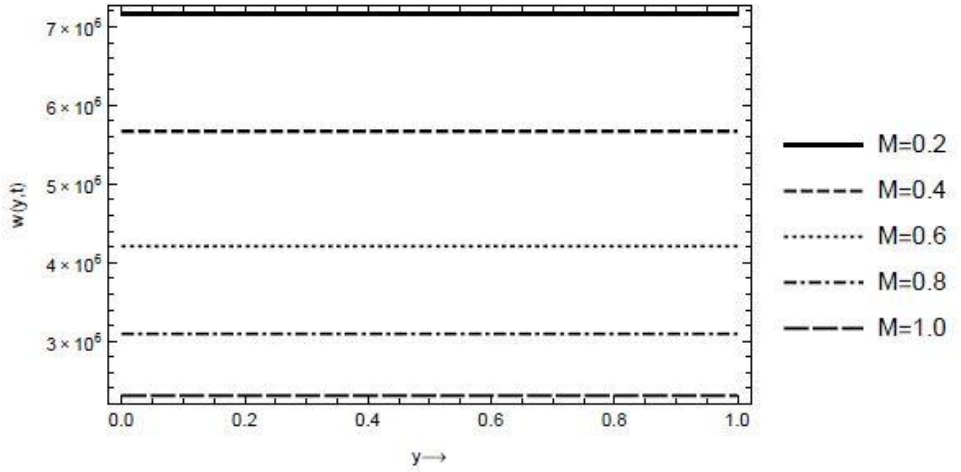

Fig 1 Velocity Profile with varying Magnetic Field and other values are
$Pr = 0.72, Da = 0.5, Ra = 50, Rs = 50, Le = 0.5, t = 5, \omega = 3, \gamma = 5$

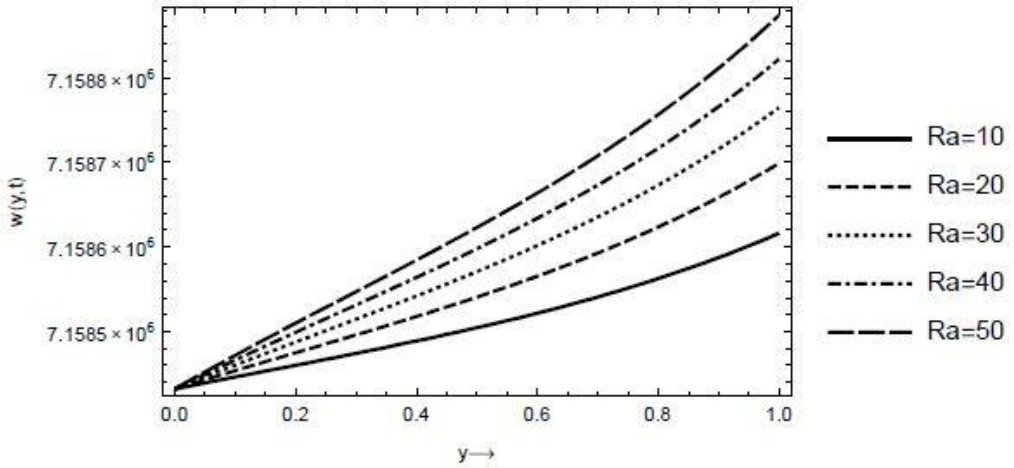

Fig 2 Velocity Profile with varying Rayleigh Number and other values are
$Pr = 0.72, Da = 0.5, M = 0.2, Rs = 50, Le = 0.5, t = 5, \omega = 3, \gamma = 5$

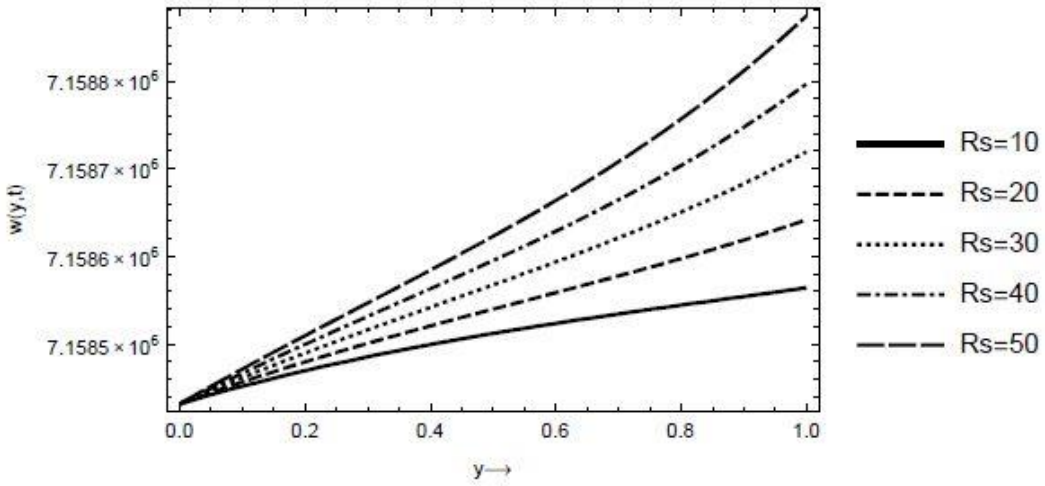

Fig 3 Velocity Profile with varying Solutal Rayleigh Number and other values are
$Pr = 0.72, Da = 0.5, Ra = 50, M = 0.2, Le = 0.5, t = 5, \omega = 3, \gamma = 5$

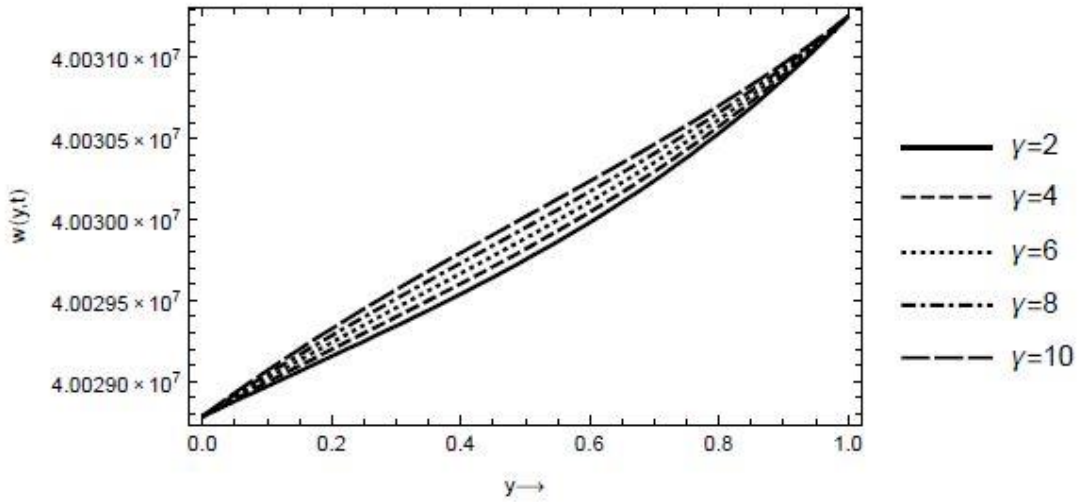

Fig 4 Velocity Profile with varying Heat Source and other values are

$Pr = 0.72, Da = 0.5, Ra = 50, Rs = 50, Le = 0.5, t = 5, \omega = 3, M = 0.2$

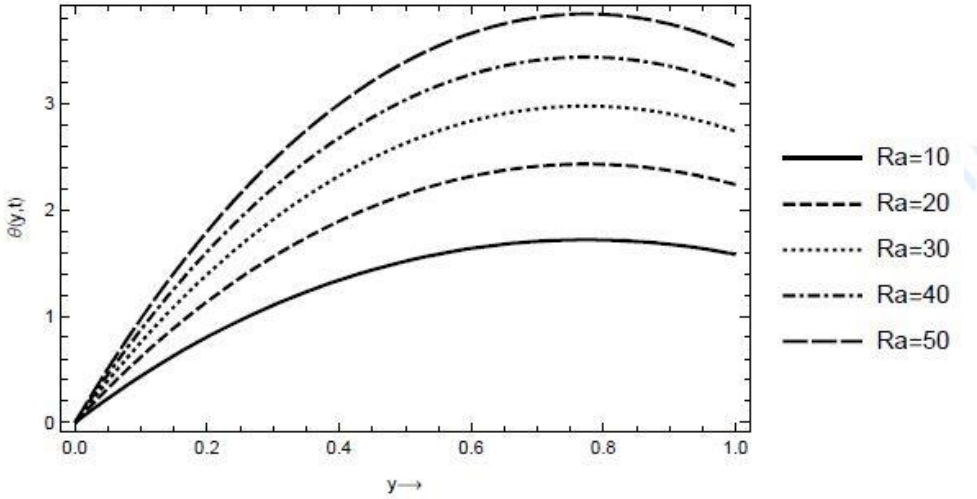

Fig 5 Temperature Profile with varying Rayleigh Number and other values are

$Le = 0.5, t = 5, \omega = 3, \gamma = 5$

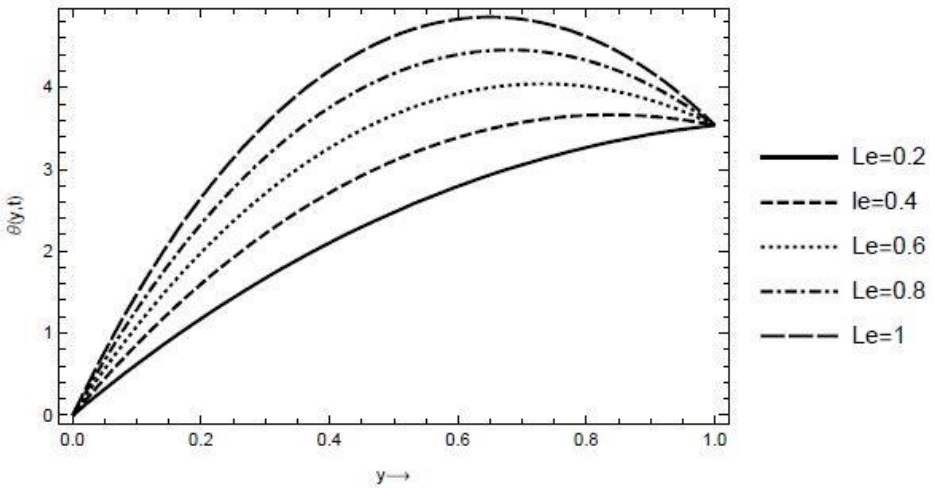

Fig 6 Temperature Profile with varying Lewis Number and other values are

$Ra = 50, t = 5, \omega = 3, \gamma = 5$

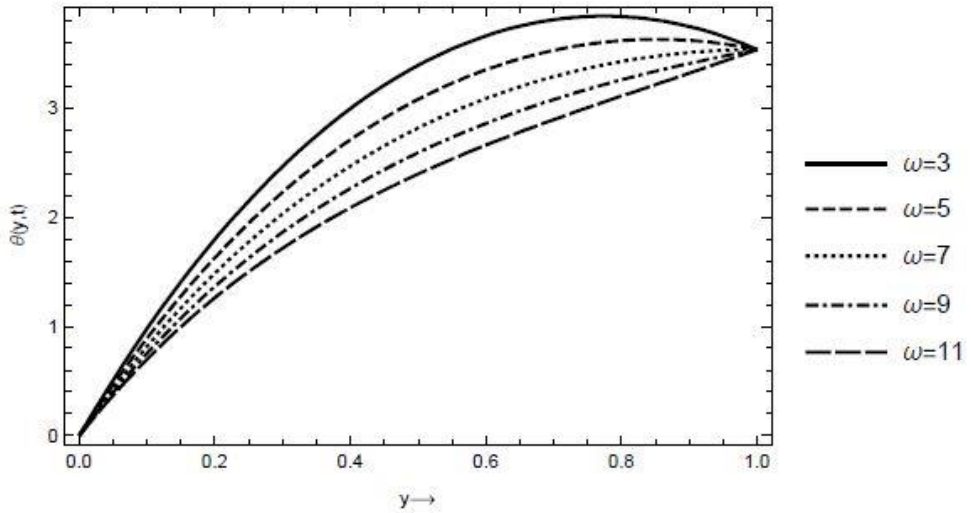

Fig 7 Temperature Profile with varying Oscillatory Frequency and other values are $Ra = 50, Le = 0.5, t = 5, \gamma = 5$

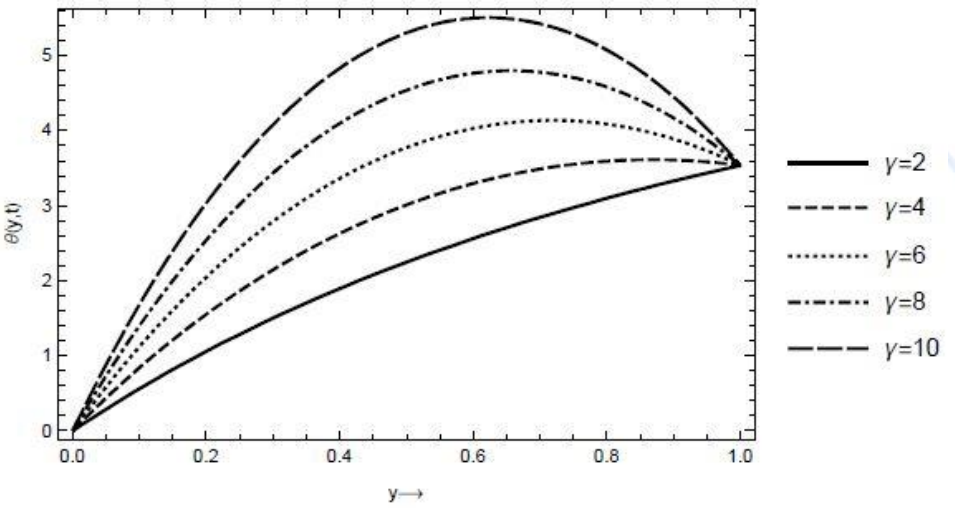

Fig 8 Temperature Profile with varying Heat Source and other values are $Ra = 50, Le = 0.5, t = 5, \omega = 3$

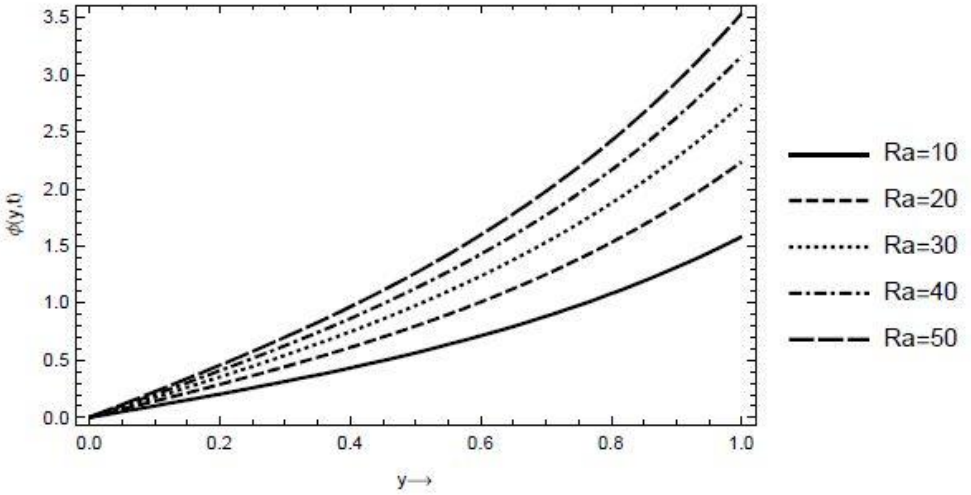

Fig 9 Concentration Profile with varying Rayleigh Number and other values are $Le = 0.5, t = 5, \omega = 3$

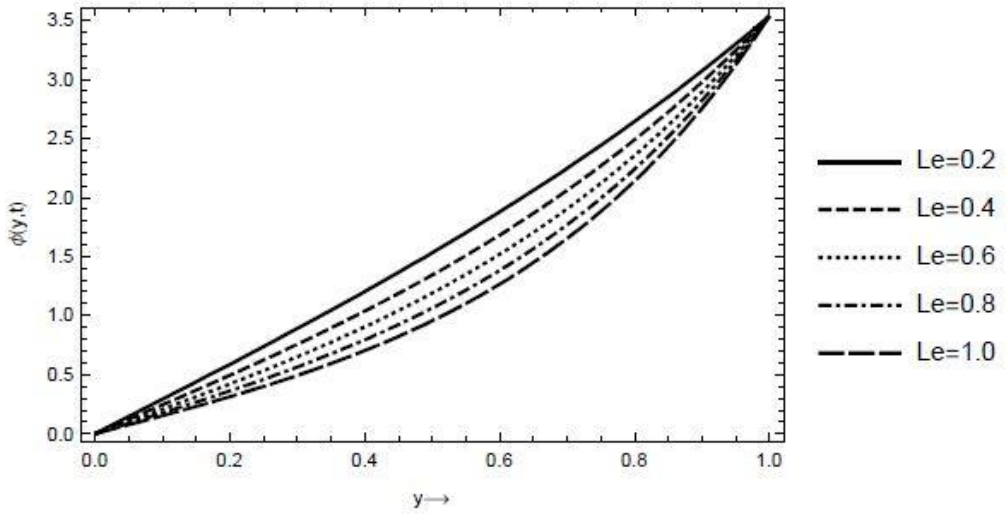

Fig 10 Concentration Profile with varying Lewis Number and other values are $Ra = 50, t = 5, \omega = 3$

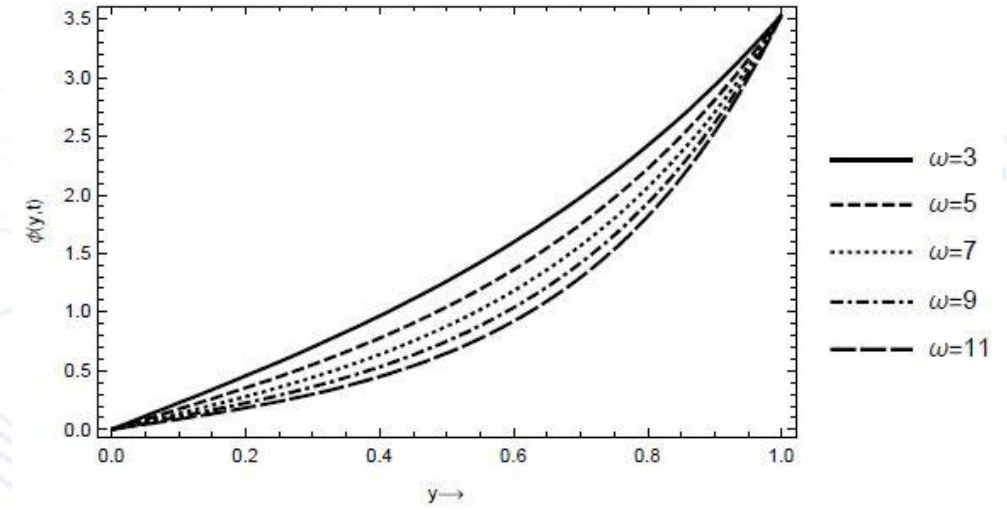

Fig 11 Concentration Profile with varying Oscillatory Frequency and other values are $Ra = 50, Le = 0.5, t = 5$

5 Discussion

In Israel-Cookey *et al*. [17] investigated the stability of the system and studied the impact of the varying parameter values on temperature and concentration profiles. However, in this article we investigated the impact of the pertinent parameters on the flow profiles, including the velocity profile. In the analytical solution, it is seen that the velocity profile exhibits a linear relationship for all the pertinent parameters. After thorough simulation, we shall discuss the results as follows:

Fig. 1 depicts the effect of the magnetic field on the fluid velocity. This result indicates that an increase in the magnetic field decreases the fluid velocity. This result typically shows the linear relationship of the parameters earlier mentioned. The Rayleigh number impact on the fluid velocity was investigated and the result is seen in Fig 2. This result is of the view that any increase in Rayleigh number increases the fluid velocity. The result of the impact of solutal Rayleigh number on the fluid velocity is shown in Fig 3. The figure shows that fluid velocity increases for an increase in solutal Rayleigh number. Figure 4 depicts the effect of a heat source on fluid velocity; this result indicates that fluid velocity increases as heat from a

source increases. The fluid involves the effect of the pertinent parameters on the fluid temperature; Fig 5 depicts an increase in fluid temperature for an increase in Rayleigh number. Fig. 6 shows a rise in fluid temperature for every increase in Lewis number. This result showed that the temperature is zero when the boundary condition is zero, and the temperature grows to a maximum level around the walls due to wall thickness. Fig. 7 shows that the fluid temperature decreases for an increase in oscillatory frequency with different maximums of the profiles. The fluid temperature increase is seen in Fig 8. This figure shows that the fluid temperature increases for an increase in heat through the source. This research also includes the impact of the pertinent parameters on the concentration of the fluid. Fig 9 demonstrates that the concentration of particles increases for an increase in Rayleigh number from 10 to 50. Fig 10 showed that the concentration in the fluid decreases for an increase in Lewis number. Finally, it is seen in Fig 11 that the specie concentration in the fluid causes an increase in oscillatory frequency.

6 Conclusion

The exact solutions of the governing equations were obtained by reducing them to ODEs using the perturbed function. The numerical simulation was carried out using Wolfram Mathematica, version 12, where the results were presented graphically. We can conclude from the results as follows:

1. The fluid velocity can be slowed down if we increase the magnetic field intensity.
2. The fluid velocity is increased if the solutal Rayleigh number and thermal Rayleigh number are increased.
3. When heat is passed through a source, the fluid velocity increases.
4. The fluid temperature can be increased if we increase the thermal Rayleigh number, the Lewis number, and the source heat, while the temperature reduces for an increase in the oscillatory frequency.
5. The specie concentration increases for an increase in thermal Rayleigh number, while the concentration reduces for an increase in Lewis number and oscillatory frequency.

References

1. Chandrasekhar, S. (1961). Hydrodynamic and Hydromagnetic Stability, Dover Publication, New York.
2. Shaowei, W., Qiangyong, Z., Zhao, M. (2014). Linear and Nonlinear stability analysis of double diffusive convection in a Maxwell fluid saturated layer with internal heat source. Journal of Applied Mathematics, 489-500.
3. Bhadauria, B.S., Hashim, I., Srivastava, A. (2014). Effects of Internal Heating on double diffusive convection ina coupled stress fluid saturated porous medium. Advances in material sciences and Applications, 3(1), 24-45.
4. Ingham, D.B., Pop, I. (1998). Transport Phenomena in porous medium, 3rd Edition, Volume III, Oxford, Elsevier
5. Nield, D.A., Bejan, A. (2006). Convection in porous media. 3rd Edition, Springer, Berlin, Germany.
6. Batchelor, G.K. (2000). An Introduction to Fluid Dynamics. Cambridge University Mathematical Library.
7. Drazin, P.G., Reid, W.H. (2004). Introduction to Hydromagnetic Stability, 2nd Edition. Cambridge University Press, Cambridge, UK.
8. Charru, F. (2011). Hydrodynamic Instabilities, Cambridge University Press, Cambridge, UK.
9. Schmid, P., Henningson, D. (2001). Stability and Transition in Shear Flows, Springer.

10. Horton, C.W., Rogers, F.T. (1945). Convention current in porous medium. Journal of Applied Physics, Vol. 16, 508-521.
11. Wooding, R.A. (1960). Convection current in porous medium. Proceedings of the Royal Society, 252-261.
12. Vafai, K. (2005). Handbook of porous media, 2nd Edition. Taylor and Francis, London.
13. Hill, A. A. (2005). Double diffusive convection in a porous medium with concentration based internal heat source, Proceedings Royal Society A461, pp. 561-574.
14. Gaikwad, S. N., Dhanraj, M. (2014). Onset of double diffusive reaction-convection in an anisotropic porous layer with internal heat source. Proceedings of the 5th International Conference on Porous media and their Applications in Science and Industry.
15. Israel-Cookey C, Ebiwareme L, Amos E. (2017). Effect of vertical magnetic field on the onset of double diffusive convection in a horizontal porous layer with concentration based internal heat source. Asian Research Journal of Mathematics, 7(1):1-15.
16. Matta, J., Hill, A. A. (2018). Double diffusive convection in an inclined porous layer with a concentration based internal heat source. Continuum Mechanics and Thermodynamics 30(1), 165-173.
17. Israel-Cookey, C., Emeka A., Ebiwareme, L. (2018). Soret and Magnetic field effects on Thermosolutal convection in a porous medium with concentration based Internal heat source. American Journal of Fluid Dynamics, 8(1), 1-6.
18. Kumar, G., Narayana, P.A.L., Chandra, K.S. (2019). Linear and nonlinear thermosolutal instabilities in an inclined porous layer. Proceedings of the Royal Society A: Mathematical Physical and Engineering Sciences, 476(2233), 20190705.
19. Ebiwareme, L., Israel-Cookey, C. (2020). Magnetic field effects on the onset of Darcy-Brinkmann convection in a thin, porous layer induced by concentration-based internal heating. Journal of Scientific and Engineering Research, 7(8), 173-184.
20. Odok, E.O., Israel-Cookey, C., Emeka, A. (2020). Onset of Magneto convection in a rotating Darcy-Brinkman porous layer Heated from below with Temperature dependent Heat source. International Journal of Mathematics Trends and Technology, Volume 66, Issue 5